Nerve Imaging in the Wrist

Steven P. Daniels, MD[1] Jadie E. De Tolla, MD[2] Ali Azad, MD[2] Catherine N. Petchprapa, MD[1]

[1] Department of Radiology, New York University Grossman School of Medicine, New York University, New York, New York
[2] Department of Orthopedic Surgery, New York University Grossman School of Medicine, New York University, New York, New York

Address for correspondence Catherine N. Petchprapa, MD, Department of Radiology, New York University Grossman School of Medicine, 333–339 East 38th Street, 6th Floor, New York, NY 10016 (e-mail: Catherine.Petchprapa@nyulangone.org).

Semin Musculoskelet Radiol 2022;26:140–152.

Abstract

Neuropathic symptoms involving the wrist are a common clinical presentation that can be due to a variety of causes. Imaging plays a key role in differentiating distal nerve lesions in the wrist from more proximal nerve abnormalities such as a cervical radiculopathy or brachial plexopathy. Imaging complements electrodiagnostic testing by helping define the specific lesion site and by providing anatomical information to guide surgical planning. This article reviews nerve anatomy, normal and abnormal findings on ultrasonography and magnetic resonance imaging, and common and uncommon causes of neuropathy.

Keywords
- wrist
- magnetic resonance imaging
- ultrasonography
- peripheral nerves
- carpal tunnel syndrome

Neuropathic symptoms involving the wrist are a common clinical presentation in both the subspecialty and primary care settings.[1,2] A detailed history and physical examination are often all that is needed for clinicians to identify the suspected lesion site. However, clinical presentations are not always stereotypical and may require further investigation. Electrodiagnostic testing can provide important information regarding the suspected lesion site, the physiologic degree of nerve injury, and the status of motor end plates, but it offers little anatomical information relevant to multiple causes of neuropathy and can provide confusing or misleading results in fascicular lesions.[3–6] Imaging is often performed as an adjunct to verify the suspected diagnosis, help identify a cause for nerve symptoms, and plan potential surgical intervention. In the wrist, both magnetic resonance imaging (MRI) and ultrasonography (US) can be used for nerve evaluation, with both modalities providing advantages depending on the suspected lesion site and pathologic condition.[7,8]

This article reviews nerve anatomy and multimodality imaging of the nerves of the wrist. We describe both common and uncommon causes of neuropathy and highlight the use of imaging in the diagnosis of carpal tunnel syndrome (CTS) and ulnar neuropathy at the wrist.

Nerve Imaging: General Considerations

Nerves are highly ordered structures consisting of bundled fascicles with surrounding fat. In the wrist, this fascicular macrostructure is most clearly demonstrated when imaging the larger median and ulnar nerves.

On MRI, nerves are intermediate signal on T1- and T2-weighted sequences and do not enhance. Because of the presence of perifascicular fat, nerves are often more readily identified on T1/proton-density (PD) images than on fat-suppressed images; T1/PD sequences can serve as a helpful roadmap during side-by-side image interpretation with T2-weighted fat-suppressed images. In general, nerves travel in fairly predictable locations and demonstrate a consistent caliber until they branch (►**Fig. 1**). MRI findings of nerve T2 signal hyperintensity, fascicular enlargement, loss of the normal fascicular appearance, or blurring of the perifascicular fat suggest abnormality. Heavily T2-weighted sequences with fat suppression optimize the identification and evaluation of small nerves and increase the conspicuity of T2 signal abnormalities.

However, because of the known magic angle effect on nerves, not all T2 signal alterations are pathologic, and unlike tendons, these orientation-dependent changes in signal intensity can persist at higher echo times and on short tau

Issue Theme Imaging Evaluation of Nerves; Guest Editor, Jenny T. Bencardino, MD

Thieme Medical Publishers, Inc., 333 Seventh Avenue, 18th Floor, New York, NY 10001, USA

DOI https://doi.org/10.1055/s-0042-1742393.
ISSN 1089-7860.

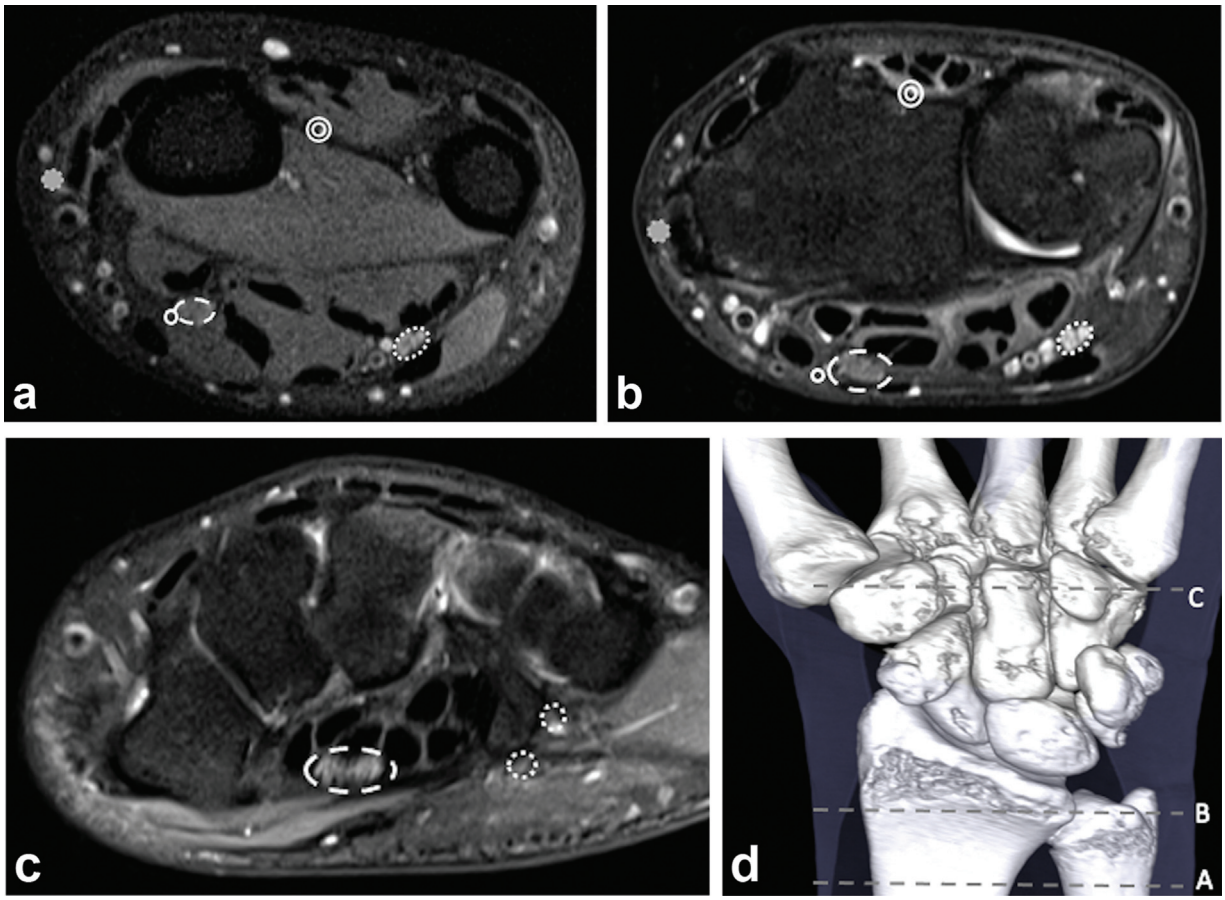

Fig. 1 (**a–c**) Expected locations of nerves in the forearm and wrist at different levels delineated by the dashed gray lines (**d**), a three-dimensional computed tomography reformat. Dashed white circle, median nerve; dotted white circle, ulnar nerve that divides into deep and superficial branches, seen in (c); small solid circle, palmar cutaneous branch of median nerve; gray circle, superficial sensory branch of radial nerve; concentric white circles, distal portion of posterior interosseous nerve.

inversion recovery sequences. A study on the effect of magic angle on 3-T MR neurography by Kästel et al, however, showed that increases in intraneural T2 signal related to magic angle were relatively mild compared with intraneural T2 signal changes in patients with clinical and electromyography (EMG)/nerve conduction velocity documented neuritis.[9] Nonetheless, angle-specific signal changes must be kept in mind when interpreting MR images, particularly when increased nerve signal intensity is the sole abnormality.

On US, nerves demonstrate a fascicular architecture with hypoechoic nerve fascicles separated by hyperechoic septae representing the interfascicular perineurium. The normal nerve demonstrates a smooth contour without areas of focal enlargement and does not demonstrate intraneural hypervascularity. Pathologic findings on US include loss of the normal fascicular architecture, intraneural hypervascularity, hypoechoic appearance of the nerve, and nerve enlargement.

US of nerves should be performed with a high-frequency linear transducer to allow for detailed evaluation. US provides several advantages over MRI, including higher spatial resolution that can be helpful when evaluating very small structures. US also allows for dynamic evaluation that can be important when assessing normal nerve gliding and the physiologic effect of perineural scarring. Although it has not been studied extensively, disadvantages of US are that it is likely less sensitive for mild nerve abnormalities (which would demonstrate T2 signal hyperintensity without nerve enlargement on MRI), and it is not as sensitive for associated muscle denervation changes that can provide clues to the suspected lesion site.

Median Nerve

Anatomy

The median nerve is a terminal branch of the brachial plexus and receives contributions from the medial and lateral cords and the C5, C6, C7, C8, and T1 nerve roots. In the upper arm, the median nerve travels medial to the axillary and brachial arteries. At the elbow, the nerve travels between the humeral and ulnar heads of the pronator teres before giving off the anterior interosseous nerve. In the forearm, the median nerve travels between the flexor digitorum profundus and flexor digitorum superficialis muscles before taking a more superficial position in the distal forearm. The median nerve usually enters the carpal tunnel radially, either superficial to the flexor digitorum superficialis tendons or between the flexor digitorum superficialis and flexor pollicis longus tendons, although nerve positioning may vary.[10] The roof

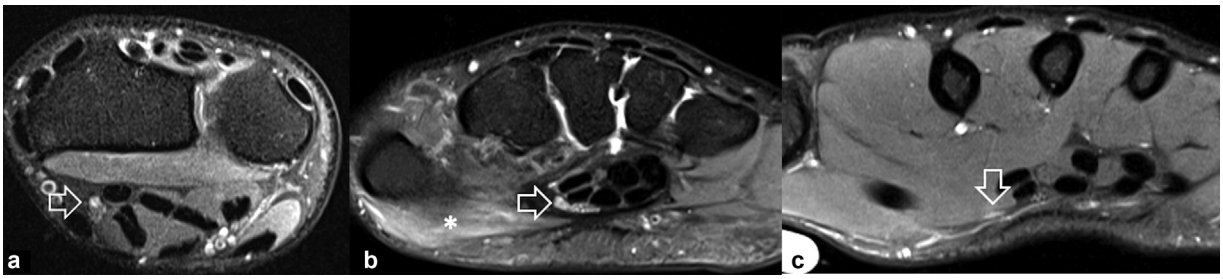

Fig. 2 A 31-year-old man with progressive weakness and thenar muscle atrophy. (**a**) Axial T2 fat-suppressed image in the distal forearm demonstrates hyperintense signal of some median nerve fascicles (white arrow). (**b**) Axial T2-fat-suppressed image at the level of the carpal tunnel also demonstrates hyperintense signal of some median nerve fascicles (white arrow), as well as denervation edema of the thenar muscles (white asterisk). (**c**) Axial T2 fat-suppressed image distal to the carpal tunnel demonstrates hyperintense signal of the recurrent motor branch of the median nerve (white arrow). At surgery, the nerve was found to be compressed by the palmar fascia, which was surgically released.

of the carpal tunnel is the flexor retinaculum, also known as the transverse carpal ligament, that attaches to the scaphoid and triquetrum proximally and the trapezium and hamate distally. The floor of the carpal tunnel is made up of the proximal and distal carpal rows. The carpal tunnel is narrowest close to the carpal tunnel outlet.

The median nerve commonly gives off a palmar cutaneous branch ~ 5 to 7 cm proximal to the radiocarpal joint. The palmar cutaneous branch originates from the radial aspect of the median nerve and travels between the flexor carpi radialis tendon and the palmaris longus tendon. This nerve enters the hand superficial to the carpal tunnel and provides sensory innervation to the volar hand over the thenar eminence.[11]

There are numerous median nerve branching patterns at and distal to the carpal tunnel.[12] It is important to be aware of variations in the course of the recurrent motor branch that innervates most of the thenar intrinsic muscles. These muscles include the abductor pollicis brevis, superficial head of the flexor pollicis brevis, and opponens pollicis (►**Fig. 2**). The most common branching pattern (46–90%) is extraligamentous. In this pattern, the recurrent motor branch divides from the median nerve distal to the flexor retinaculum off the radial side at or just distal to the origin of the common palmar digital nerve to the thumb. The nerve can also originate deep to the flexor retinaculum and travel distal to the flexor retinaculum (subligamentous) or through the flexor retinaculum (transligamentous) before innervating the thenar muscles. Rarely, the recurrent branch can originate from the ulnar aspect of the median nerve distal to the carpal tunnel. Accessory motor branches can also be present.[12,13]

Within the carpal tunnel, the median nerve can also have a variable appearance. An early bifurcation of the median nerve or bifid median nerve is a common anatomical variant. Some studies showed an increased prevalence of a bifid median nerve in patients with CTS compared with volunteers; other studies showed a similar prevalence.[14,15] The prevalence of a bifid median nerve in these studies ranges from 10% to 20%. A persistent median artery is a common vascular variant occurring in ~ 10 to 15% of the population.[16] Studies show an increased prevalence of this variant in cases of bifid median nerve, where it occurs in ~ 45 to 65% of cases.[14,17]

Normal Imaging Appearance

The median nerve is well evaluated with either US or MRI. On US, the normal median nerve has maintained fascicular architecture and a consistent caliber as it travels through the distal forearm and carpal tunnel. Toggling the transducer causes the adjacent flexor tendons to undergo anisotropy while the nerve maintains a more consistent echogenicity. US evaluation of the median nerve should include cross-sectional area measurements at the level of the proximal third of the pronator quadratus and within the carpal tunnel. The normal median nerve demonstrates a mean cross-sectional area (CSA) of 9 mm^2 within the carpal tunnel and a change in CSA < 2 mm^2 when comparing the CSA in the carpal tunnel with that of the distal forearm.[18]

On MRI, the normal median nerve demonstrates intermediate T1 and T2 signal with maintained internal fascicular architecture and smooth contour without caliber change as it courses through the distal forearm and carpal tunnel. Studies showed the CSA of the median nerve measured on MRI to be consistently larger than US and to better correlate with cadaveric measurements.[19] A recent study showed average CSA of the median nerve just proximal to the carpal tunnel inlet to be ~ 11.2 mm^2 in asymptomatic patients.[20]

Carpal Tunnel Syndrome

CTS is the most common compressive neuropathy in the upper extremity and accounts for > 500,000 surgical procedures performed annually in the United States.[21] Patients commonly present with paresthesia and/or intermittent numbness in the median nerve distribution of the hand and can have pain in the thenar eminence. Nocturnal symptoms are common, and patients frequently complain of painful nighttime paresthesias. In advanced cases, patients may demonstrate constant numbness and weakness with associated atrophy of the thenar musculature. Symptoms usually worsen during the night. Early diagnosis and treatment is key to preventing irreparable median nerve damage and permanent sensory and motor changes. Initial nonoperative management often consists of nighttime splinting and/or nerve glide exercises.[22] Corticosteroid injections can act as both a therapeutic and diagnostic tool. Patients who fail to respond to conservative management or present

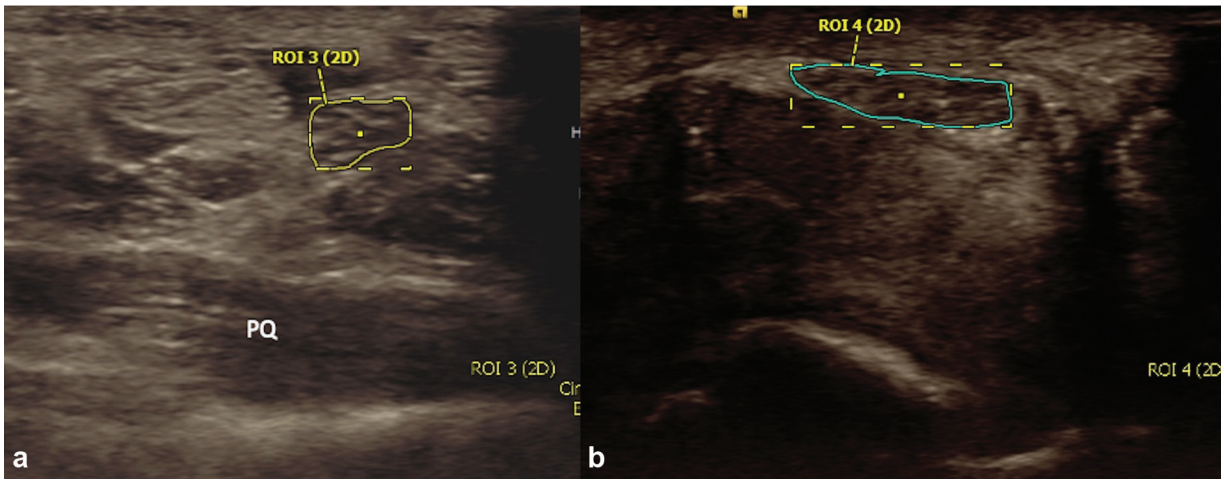

Fig. 3 A 71-year-old man with pain in the median nerve distribution and concern for carpal tunnel syndrome. (**a**) Transverse ultrasonography (US) image at the level of the proximal pronator quadratus (PQ) demonstrates a median nerve cross-sectional area of 7.5 mm^2. ROI, region of interest. (**b**) Transverse US image at the level of the carpal tunnel demonstrates a flattened appearance of the median nerve with cross-sectional area of 14 mm^2. The difference of >2 mm^2 in the cross-sectional area suggests carpal tunnel syndrome with high sensitivity and specificity.

with weakness and significant sensory changes are treated with carpal tunnel release that can be performed using open or endoscopic techniques.

Although CTS is mainly a clinical diagnosis, electrodiagnostic testing can be helpful in confirming the diagnosis, as well as assessing the severity of nerve injury and ruling out other processes such as cervical radiculopathy or a more diffuse polyneuropathy.[23] Although previously considered the gold standard for establishing the diagnosis of CTS, studies show electrodiagnostic testing to have false positives and false negatives, and many clinicians do not routinely order electrodiagnostic testing in clinically unambiguous cases.[24,25]

US of the median nerve has been studied extensively in cases of suspected CTS.[26,27] A 2014 article comparing US with electrodiagnostic testing using a clinical tool as the reference standard showed US to have a sensitivity of 89% and specificity of 90% compared with 89% and 80% for electrodiagnostic testing.[26] Numerous imaging criteria have been described in the literature for evaluating median nerve size and morphology.[18,28] In general, CTS results in enlargement of the median nerve CSA within the carpal tunnel. A 2009 article by Klauser et al showed that using a CSA threshold of 12 mm^2 in the carpal tunnel resulted in a sensitivity of 94% and specificity of 95% in identifying patients with CTS using electrodiagnostic testing as a gold standard.[18] In the same study, a threshold of 10 mm^2 resulted in 100% sensitivity but only 57% specificity. Importantly, the same study also looked at the differences in CSA within the carpal tunnel compared with at the level of the proximal pronator quadratus in the distal forearm. Patients with CTS demonstrated a change in CSA of 7.4 mm^2 on average versus 0.25 mm^2 in healthy volunteers. Using 2 mm^2 as a threshold resulted in a sensitivity of 99% and specificity of 100% in identifying patients with CTS (►**Fig. 3**). These are the criteria used predominantly in our practice.

A follow-up study in 2015 showed the degree of increased CSA within the carpal tunnel compared with at the level of the pronator quadratus to correlate well with the severity of disease on nerve conduction studies.[29] Assessment of nerve CSA can be complicated if there is bifid median nerve morphology. In these cases, CSA can be calculated by manually tracing both nerve components and adding the areas together. Using a nerve CSA of 12 mm^2 in the carpal tunnel results in a sensitivity of 83 to 87%, although a specificity of only 43 to 50%.[30] Comparing the CSA of a bifid median nerve within the carpal tunnel versus at the level of the proximal pronator quadratus, however, yields better results. Using a change in CSA threshold of 4 mm^2 results in a sensitivity of 93% and a specificity of 93 to 96% in identifying patients with CTS.[30]

Other imaging signs have been evaluated in the setting of CTS. Palmar bowing of the flexor retinaculum has been measured at the level of the hamate and trapezium. Studies presented mixed results with one study showing 2 mm of palmar bowing to have a 44% sensitivity and 85% specificity in identifying patients with CTS.[31,32] Other studies showed palmar bowing at the carpal tunnel inlet (between the scaphoid and pisiform) to be a specific sign of CTS with a threshold of 1 mm demonstrating a specificity of 97%.[28] Median nerve hypervascularity on Doppler US is a specific although insensitive sign of CTS, with one study demonstrating a sensitivity of 69% and specificity of 95%.[32] Flattening ratio is the length of the major nerve axis divided by the minor axis and can be measured at either the proximal or distal carpal tunnel. Cutoffs of 2.5 and 3 have been used, and in general, flattening ratio is not a sensitive or specific sign for identifying cases of CTS.[28,31,32] Median nerve CSA can also be measured just distal to the carpal tunnel outlet with one study showing a CSA >14 mm^2 to have a sensitivity of 64% and specificity of 100% in identifying cases of CTS.[28]

MRI is less commonly performed for suspected CTS and has been less extensively studied than US. Compression of the median nerve in the carpal tunnel leads to vascular congestion, neural edema, and a blockage of axoplasmic flow, contributing to T2 hyperintense signal (►**Fig. 4**).[33]

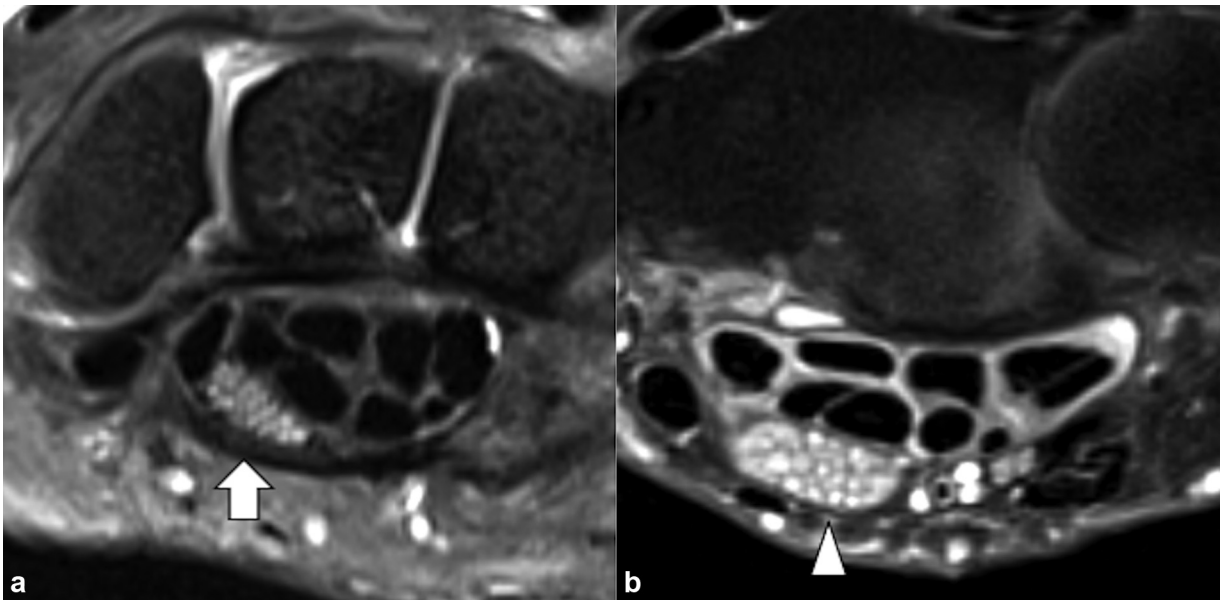

Fig. 4 Variations in median nerve signal. (**a**) Axial T2 fat-suppressed image in a 41-year-old woman with ulnar-sided wrist pain and no clinical neuritis demonstrates a normal median nerve with intermediate signal fascicles and no nerve enlargement (white arrow). (**b**) Axial T2 fat-suppressed image in a 71-year-old woman with carpal tunnel syndrome demonstrates hyperintense enlarged nerve fascicles, contributing to a significant enlargement of the median nerve (white arrowhead).

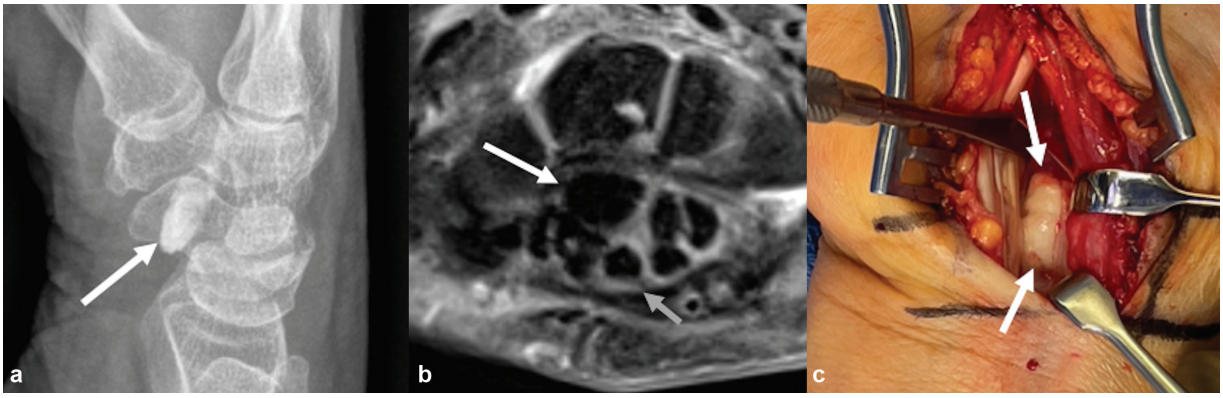

Fig. 5 A 75-year-old woman with 8 months of right hand numbness, tingling, and weakness. (**a**) Initial lateral radiograph of the wrist demonstrates calcification projecting over the carpal tunnel (white arrow). (**b**) Axial proton-density fat-suppressed image demonstrates a low signal mass deep within the carpal tunnel (white arrow), contributing to compression of the median nerve against the flexor retinaculum (gray arrow). (**c**) Intraoperative image at the time of carpal tunnel release and mass excision demonstrates a calcified mass deep within the carpal tunnel (white arrows). Final pathology showed tumoral calcinosis, and the patient's symptoms improved significantly after surgery.

Increased median nerve signal relative to the signal of the hypothenar muscles was shown to occur more commonly in patients with carpal syndrome than controls with a signal intensity ratio threshold of 1.05 demonstrating a sensitivity of 88% and specificity of 68% for identifying positive cases.[20] A median nerve CSA of either 15 mm^2 just proximal to the carpal tunnel inlet or 15 mm^2 just distal to the carpal tunnel outlet provides a sensitivity of 100% and a specificity of 94% in diagnosing CTS.[20]

Both MRI and US can be used to identify secondary causes of CTS. Space-occupying lesions causing CTS occur in ~ 3% of cases with causes including radial or ulnar bursitis, radiocarpal synovitis, anomalous muscles, gout, and masses such as ganglion, lipoma, fibroma of the tendon sheath, and tumoral calcinosis (►**Fig. 5**).[34] It is important to identify masses contributing to CTS so they can be addressed at the time of carpal tunnel release. Anomalous muscles in or adjacent to the carpal tunnel include variations in the palmaris longus muscle, such as distal muscle tissue, palmaris profundus muscle, proximal origin of a lumbrical muscle, and a digastric flexor digitorum superficialis tendon.[35,36] CTS can be an early presentation of amyloidosis and can occur years before cardiac involvement.[37] Imaging findings suggestive of amyloidosis include heterogeneous synovial thickening with nodular areas of low T2 signal and osseous erosions (►**Fig. 6**). If present, it is important to raise suspicion for amyloidosis, so biopsy can be performed at the time of carpal tunnel release and early treatment can be initiated to prevent cardiac and multiorgan involvement.

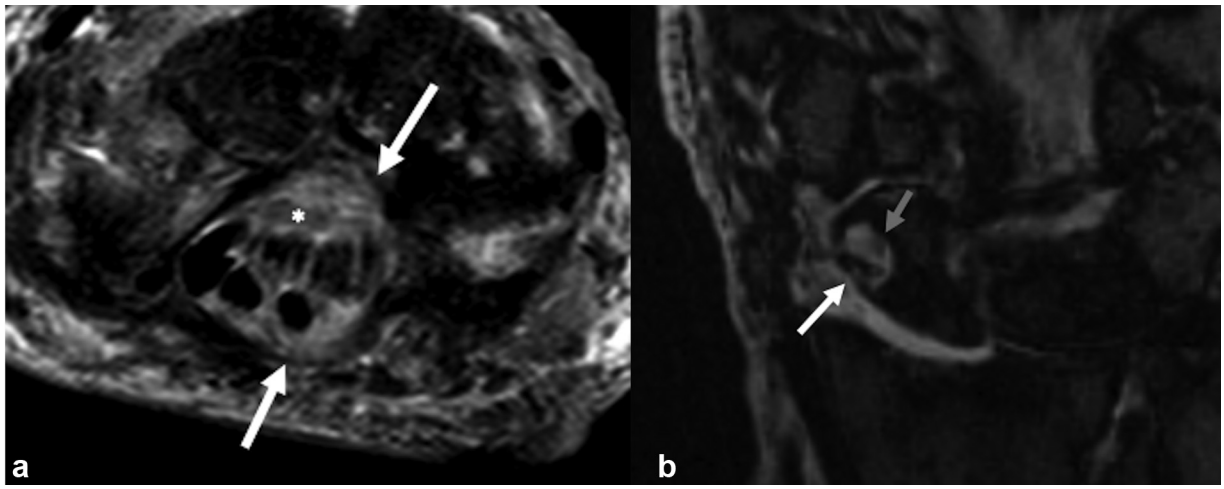

Fig. 6 A 78-year-old man with multiple myeloma and amyloidosis who presented with right hand pain concerning for carpal tunnel syndrome. (**a**) Axial T2 fat-suppressed image demonstrates heterogeneous synovitis involving the ulnar bursa (white arrows) with areas of low signal (white asterisk). (**b**) Coronal short tau inversion recovery image demonstrates large erosion within the scaphoid (white arrow) including areas of low signal (gray arrow).

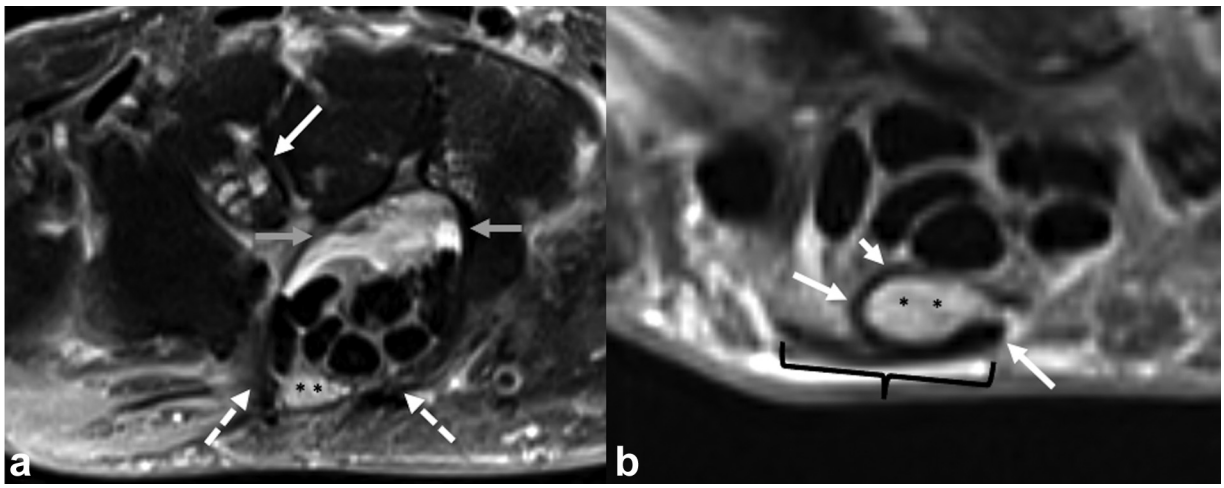

Fig. 7 A 68-year-old woman with ongoing numbness after carpal tunnel release 4 months earlier. (**a**) Axial T2 fat-suppressed image demonstrates a gap in the transverse carpal ligament (dashed white arrows) and a hyperintense median nerve (black asterisks). Findings of midcarpal arthritis (white arrow) and associated synovitis (gray arrows) are also present. (**b**) A more proximal axial T2 fat-suppressed image demonstrates near-circumferential hypointense fibrosis (white arrows) around the hyperintense median nerve (black asterisks). The fibrosis is adherent to the overlying palmar retinaculum (black bracket). The patient underwent subsequent neurolysis with improvement of symptoms.

Residual or recurrent symptoms after carpal tunnel release pose a difficult challenge for the treating physician. The most common causes of symptoms are incomplete release of the flexor retinaculum and perineural scarring/fibrosis.[38] Imaging signs of perineural fibrosis include intermediate/low signal or hypoechoic perineural tissue and ill-defined nerve margins (►**Fig. 7**). This is important to identify because scarring often requires neurolysis, and some surgeons use a vein graft or a hypothenar fat graft to decrease the risk of recurrent scarring after surgery.[38] Caution should be used when interpreting the flexor retinaculum because the retinaculum was shown to reconstitute in more than half of patients at 12 months, even in patients with good clinical outcomes.[39] An intact retinaculum outside of the early postoperative period should not be interpreted as an incomplete release but rather a reconstituted or intact retinaculum. Similarly, caution should be used when interpreting nerve CSA/morphology as a sign of recurrent or residual nerve compression because the nerve can remain abnormal in size for >12 months after release.[39]

Ulnar Nerve

Anatomy

The ulnar nerve is the terminal branch of the medial cord of the brachial plexus and receives contributions from the C8 and T1 nerve roots. The nerve travels posteromedial to the brachial vessels in the anterior compartment of the upper arm before piercing the medial intermuscular septum at the arcade of Struthers and entering the posterior compartment where it travels along the medial head of the triceps. At the elbow, the nerve travels posterior to the medial epicondyle and enters the

cubital tunnel, a common site of compressive neuropathy. The ulnar nerve then travels between the humeral and ulnar heads of the flexor carpi ulnaris muscle before passing through the flexor pronator aponeurosis. In the forearm, the nerve lies between the flexor digitorum superficialis and flexor digitorum profundus muscles; in the distal forearm, it is deep to the flexor carpi ulnaris, where it is relatively protected and becomes superficial distal to the myotendinous junction in the wrist. In the distal forearm, the ulnar nerve gives off dorsal and palmar cutaneous branches that innervate the dorsal and palmar aspects of the ulnar hand, respectively.

The ulnar nerve and ulnar artery enter the palm via Guyon's canal at the wrist. Guyon's canal is triangular and $\sim$ 4 cm in length. Its proximal, ulnar, and distal/radial margins are defined by the proximal edge of the volar (palmar) carpal ligament, which is the thickened continuation of the antebrachial fascia, the pisiform and the fibrous arch of the hypothenar muscles, and the hook of the hamate, respectively. The transverse carpal, pisohamate, and pisotriquetral ligaments form the floor. The volar carpal ligament, palmaris brevis muscle, and hypothenar connective tissue form the roof. Although sometimes variable, the ulnar nerve commonly divides into a superficial sensory branch and a deep motor branch within Guyon's canal at the level of the distal pisiform.[40] The superficial sensory branch provides motor innervation to the palmaris brevis muscle as it continues distally, superficial to the hypothenar muscles, before branching into the third common digital nerve and the ulnar proper digital nerve of the small finger. The deep motor branch travels beneath a fibrous arch of the hypothenar muscles and directly ulnar to the hook of the hamate before coursing radially within the deep palmar space to innervate the hypothenar muscles, the third and fourth lumbricals, the dorsal and palmar interossei, the adductor pollicis, and a portion of the flexor pollicis brevis.

Normal Imaging Appearance

Both US and MRI can be used effectively to image the ulnar nerve at the distal forearm and wrist.[41,42] On US, the mean CSA of the nerve within Guyon's canal is 6 mm^2 for men and 5 mm^2 for women without significant side-to-side variability in the same individual.[42] Although not yet extensively studied, some physicians use 8 mm^2 as an upper limit of normal for the ulnar nerve CSA within Guyon's canal.[42,43] The deep motor and superficial sensory ulnar nerve branches can be identified as small hypoechoic structures with mean CSAs of 2 mm^2 and 3 mm^3, respectively.[42] The ulnar artery should demonstrate normal flow on color Doppler imaging without evidence of focal enlargement to suggest thrombosis.

On MRI, the ulnar nerve maintains a consistent caliber throughout its course in the distal forearm and at the wrist. Similar to the median nerve, the ulnar nerve should demonstrate isointense to slightly hyperintense signal when compared with the adjacent muscle on fat-suppressed T2-weighted sequences. A 1992 article studying 36 wrists demonstrated a mean ulnar nerve diameter of 3 mm within Guyon's canal.[44] However, there are no well-defined criteria for an enlarged ulnar nerve on MRI.

Guyon's Canal Syndrome

Guyon's canal syndrome, or ulnar nerve entrapment at the wrist, is an uncommon condition with the incidence not well documented. Patients present with decreased grip and pinch strength and/or altered sensation in the hypothenar region or ring or small fingers.[45] Patients may present with a history of repetitive direct compression of the wrist, such as gripping the handlebars of a bicycle or operating heavy machinery, and they may also present after acute trauma.[46]

Guyon's canal is commonly divided into three zones that explain the varying presentations of Guyon's canal syndrome based on the branching pattern of the ulnar nerve.[47] Zone 1 extends from the proximal edge of the palmar carpal ligament to the ulnar nerve bifurcation. It contains both motor and sensory fascicles. Thus lesions in this location usually produce combined motor and sensory symptoms. The sensory nerve fascicles are volar to the motor fascicles in zone 1; superficial lesions often produce sensory symptoms before motor symptoms; the opposite is true of deep lesions.[47] Zone 2 extends from the ulnar nerve bifurcation to the fibrous arch of the hypothenar muscles. Because it contains the deep motor branch, zone 2 lesions usually result in only motor symptoms. Zone 3 extends from the ulnar nerve bifurcation to the exit of the canal and includes the superficial sensory branch; therefore, a lesion in this zone usually produce only sensory symptoms.[47]

Electrodiagnostic testing can be helpful in differentiating Guyon's canal syndrome from ulnar neuropathy at the elbow or cervical radiculopathy and can also identify signs of motor neuron disease or diffuse peripheral neuropathy.[48] In cases with motor symptoms, needle EMG can help narrow the suspected lesion site by identifying patterns of denervation changes in the hypothenar, interosseous, and thenar muscles.[49]

Both US and MRI can be used in suspected Guyon's canal syndrome to evaluate nerve size and morphology as well as to identify mass lesions. Signs of Guyon's canal syndrome on US include enlargement of the ulnar nerve, loss of the normal fascicular architecture, or focal change in nerve caliber.[43] MRI can demonstrate these findings in addition to T2 hyperintense nerve signal.[50] MRI can also identify denervation changes in the affected muscles of the hand.[8] Numerous causes of Guyon's canal syndrome have been described including fractures, particularly of the hook of the hamate, ganglia, anomalous muscles, thickened surrounding ligaments, and ulnar artery thrombosis (►**Fig. 8**).[45,47]

Anomalous muscles around Guyon's canal are well described.[44,51] Most often, these are variations in the abductor digiti minimi muscle that originates from the pisiform and is directly adjacent to the ulnar nerve within Guyon's canal.[44] Muscle variations are seen commonly in asymptomatic patients.[52] Some surgeons believe that larger sized accessory muscles may contribute to causing Guyon's canal syndrome, although further research is necessary to verify this idea.[53]

In general, Guyon's canal syndrome secondary to repetitive trauma is treated nonsurgically though activity modification. Patients with weakness, muscle denervation, atrophy, and persistent sensory symptoms are generally treated surgically. At surgery, the ulnar nerve is exposed from the distal forearm through the entire Guyon's

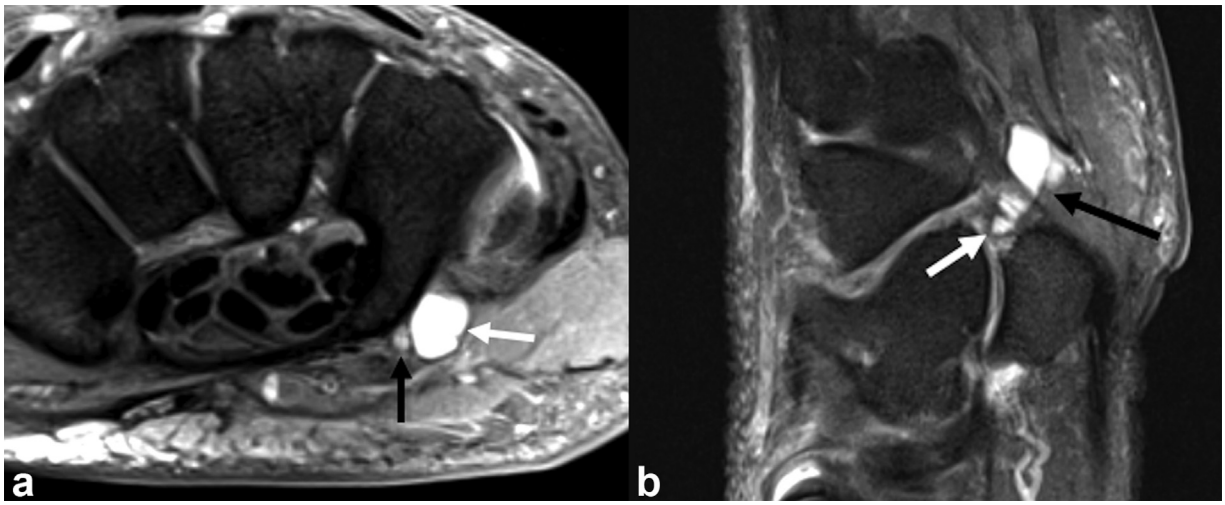

Fig. 8 A 58-year-old man with 4 months of left hand weakness without pain. (**a**) Axial proton-density (PD) fat-suppressed image demonstrates a ganglion (white arrow) compressing the hyperintense motor branch of the ulnar nerve (black arrow) adjacent to the hook of the hamate. (**b**) Sagittal PD fat-suppressed image demonstrates the ganglion (black arrow) with neck extending to the pisotriquetral joint (white arrow).

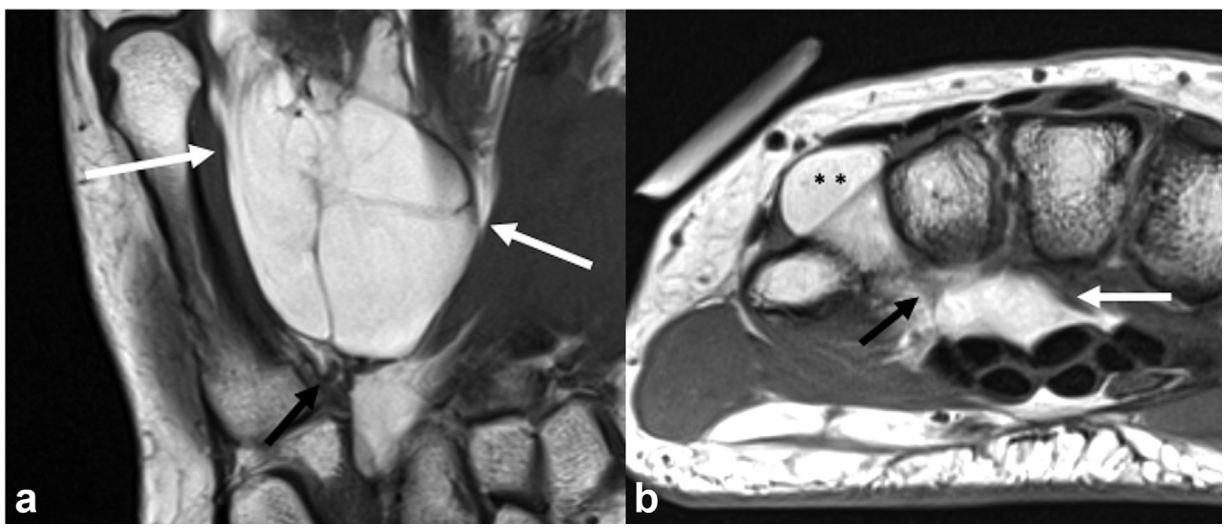

Fig. 9 A 67-year-old man with a left hand mass. Imaging was obtained to evaluate the extent of the mass and relationship to the deep branch of the ulnar nerve. (**a**) Coronal T1 image demonstrates a fat-containing mass in the palm in close proximity to the deep branch of the ulnar nerve (black arrow). (**b**) Axial T1 image demonstrates the mass (white arrow) displacing the deep branch of the ulnar nerve (black arrow) and extending into the dorsal soft tissues (black asterisks).

canal.[54] Ganglions should be resected in their entirety including all articular extensions, and the joint of origin should be debrided to prevent cyst recurrence. Outcomes after Guyon's canal decompression are excellent, although symptoms can persist if all sites of compression are not addressed.[55]

Deep Branch of Ulnar Nerve Compression

The deep motor branch of the ulnar nerve can be compressed distal to Guyon's canal as it courses radially though the palm (►**Fig. 9**). Patients present with motor symptoms, often sparing the hypothenar muscles, which are usually innervated before the ulnar nerve exits Guyon's canal. Muscles affected include the third and fourth lumbricals, interosseous muscles, adductor pollicis, and deep portion of the flexor pollicis brevis, depending on the lesion site.[56] The most common cause of compression is a ganglion, and MRI can help identify it and its origin as well as define its relationship to the deep branch of the ulnar nerve for surgical planning.[57]

Radial Nerve

Anatomy

The radial nerve is a terminal branch of the posterior cord of the brachial plexus and receives contributions from the C5, C6, C7, C8, and T1 nerve roots. After traveling through the posterior axilla, the nerve crosses medial to lateral along the posterior aspect of the humeral diaphysis at the spiral groove. The radial nerve then pierces the lateral

intermuscular septum at the level of the distal humerus, at least 7.5 cm above the distal humerus articular surface, and travels anterior to the lateral epicondyle. At the level of the radiocapitellar joint, the nerve divides into a superficial sensory branch and a deep motor branch.

The superficial sensory branch travels deep to the brachioradialis muscle in the proximal and mid forearm before piercing the superficial fascia and becoming subcutaneous ~ 5 to 10 cm proximal to the radial styloid where it lies between the brachioradialis and extensor carpi radialis longus. The nerve then courses adjacent to the first extensor compartment to the dorsum of the hand, providing sensory innervation to the radial aspect of the hand and dorsal aspect of the thumb, index finger, middle finger, and radial aspect of the ring finger.

The deep motor branch travels under the arcade of Frohse between the superficial and deep heads of the supinator muscle where it becomes the posterior interosseous nerve. The posterior interosseous nerve then exits the radial tunnel and travels through the forearm where it innervates the posterior compartment muscles. Distally, the terminal branch of the posterior interosseous nerve can be found on the floor of the fourth dorsal extensor compartment. It provides sensory innervation to the dorsal wrist capsule.

Normal Imaging Appearance

The normal superficial radial nerve can be imaged with US in the distal forearm where the nerve travels close to the cephalic vein. The normal nerve is small, measuring ~ 2 mm^2 in CSA and containing about two to six fascicles that may not be visible on imaging.[58,59] In cases of suspected of suspected nerve abnormality, comparison with the contralateral side is helpful to identify subtle lesions. With MRI the nerve appears as a small intermediate signal structure.[7] Importantly, the nerve should maintain a smooth contour without focal enlargement or surrounding edema.

The terminal branch of the posterior interosseous nerve is rarely perceptible with imaging. The nerve is usually near the scapholunate ligament and demonstrates a variable branching pattern.[60] The proximity of the nerve to the dorsal wrist capsule, scapholunate ligament, and fourth dorsal extensor compartment tendons is likely a contributing factor to dorsal wrist pain when ganglia develop in this region.[61]

Wartenberg's Syndrome

Wartenberg's syndrome, or cheiralgia paresthetica, is neuropathy of the superficial radial nerve that often presents with pain along the dorsal radial aspect of the hand.[62] The cause can be compression of the nerve between the brachioradialis and extensor carpi radialis longus tendons in the distal forearm, variant nerve course, injury during cephalic vein cannulation, mass lesion along the nerve course, or external compression from a wristwatch or handcuffs.[63,64] Irritation of the nerve can also occur in cases of de Quervain's tenosynovitis.[65]

Both US and MRI can demonstrate an abnormal nerve course, focal nerve caliber change, and surrounding soft tissue edema (►**Fig. 10**). MRI can also demonstrate T2 hyperintense signal of the nerve, suggesting injury/neuritis. The first extensor compartment should be evaluated concurrently for signs of tenosynovitis that may be the primary pathologic condition.

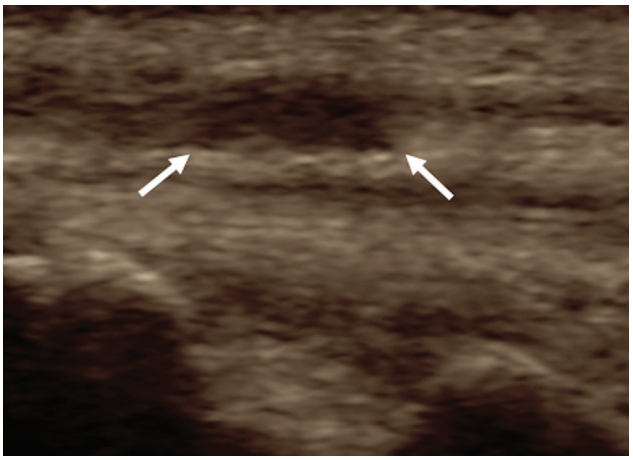

Fig. 10 A 30-year-old woman with hyperesthesia in the distribution of the left superficial radial nerve after prior wrist fusion. Longitudinal ultrasonography image demonstrates focal enlargement of the superficial radial nerve (white arrows) consistent with a neuroma-in-continuity.

Other Nerve Pathologic Conditions

Fibrolipomatous Hamartoma

Fibrolipomatous hamartoma is a benign tumor resulting from proliferation of mature adipocytes within the nerve sheath and perineural and epineural fibrosis. The proliferation of fatty tissue leads to nerve enlargement and often to spreading out of the nerve fascicles.[66] Patients often present with pain and paresthesias that can mimic a compression neuropathy, and some patients develop macrodactyly.[66] The median nerve is most commonly involved, although involvement of several other nerves, including the ulnar and radial nerves, has been described.[67]

MRI demonstrates enlargement of the nerve with thickening of nerve fascicles and increased intraneural fat that can be between or around the nerve fascicles (►**Fig. 11**).[68] There is usually no contrast enhancement, and the nerve fascicles demonstrate normal signal on T2 fat-suppressed sequences. The identification of increased fat within the nerve sheath allows for a confident diagnosis, and tissue sampling is rarely indicated. US typically demonstrates enlargement of the nerve with thick hypoechoic fascicles surrounded by prominent echogenic fat.[67]

Benign Peripheral Nerve Sheath Tumors

Benign peripheral sheath tumors include neurofibromas and schwannomas and occur throughout the body. Tumors can occur sporadically, as well as in genetic syndromes such as neurofibromatosis type 1 and type 2. Patients can present with a variety of symptoms including pain, paresthesias/numbness, weakness, and a palpable mass. Benign peripheral nerve sheath tumors have a similar appearance throughout the body. On US, they appear as hypoechoic masses along the course of the nerve and can demonstrate areas of internal hypervascularity as well as posterior acoustic enhancement.[69]

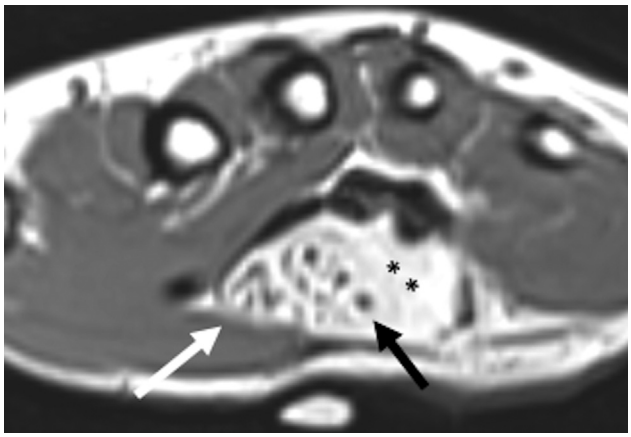

Fig. 11 An 18-year-old woman with 2 months of pain and numbness in the median nerve distribution of her right hand. Axial T1 image demonstrates enlargement of the median nerve (white arrow) with intraneural fat (black asterisks) leading to separation of the nerve fascicles (black arrow). The nerve was normal in signal on T2 fat-suppressed images (not shown).

On MRI, peripheral nerve sheath tumors appear as fusiform lesions along the course of the nerve with low to intermediate T1 signal, hyperintense T2 signal, and contrast enhancement. Several signs have been described to help identify benign peripheral nerve sheath tumors including the target sign, fascicular sign, and the split fat sign (►**Fig. 12**).[70] The radiologist's report plays a vital role in patient management when masses are present along the nerve course in the hand and wrist. Asymptomatic masses are not always resected if characteristic imaging features of a benign peripheral nerve sheath tumor are present. With symptomatic tumors, it is important to mention the possibility of a nerve sheath tumor so patients can be counseled preoperatively about potential deficits after resection.

Traumatic Nerve Injury

About 3% of trauma patients experience a peripheral nerve injury, and nerves of the hand and wrist are commonly injured due to their superficial location.[71] The Sunderland classification is commonly used to classify nerve injuries and help guide management.[72] Imaging with either US or MRI plays a key role at our institution in helping differentiate higher grade injuries that will require surgical intervention from injuries that can be treated nonoperatively.

In a Sunderland grade 1 injury, or neuropraxia, the myelin sheath is injured, although the nerve remains structurally intact with intact axons, endoneurium, perineurium, and epineurium. MRI can demonstrate T2 hyperintense nerve signal; US findings may be normal or demonstrate nerve hypoechogenicity. Sunderland grade 2 and 3 injuries, or axonotmesis, describe injury to the axons and axons plus endoneurium, respectively. MRI can demonstrate T2 hyperintense nerve signal with diffuse nerve enlargement and effacement of the nerve fascicles. US may demonstrate nerve hypoechogenicity, diffuse nerve enlargement, and loss of the normal fascicular architecture. In grade 3 injuries, recovery can be prolonged, and scarring may need to be surgically released around the swollen nerve fascicles.[73]

Sunderland grade 4 injuries include injury to the structures involved in grade 3 injuries with additional injury to the perineurium. Both MRI and US demonstrate focal nerve enlargement at the injury site, termed a neuroma-in-continuity. Nerve fascicles appear disrupted with loss of normal internal architecture. Importantly, the epineurium remains intact, and there is no gap between the nerve ends. Sunderland grade 5 injuries, or neurotmesis, are complete nerve transections with disruption of the epineurium. Both Sunderland grade 4 and grade 5 injuries require surgical intervention for meaningful recovery.[74] Sunderland grade 6, or mixed nerve injuries, involve different portions of the nerve connective tissue across the nerve cross section and include partial lacerations (►**Fig. 13**). Importantly, electrodiagnostic testing is unable to differentiate axonotmesis (Sunderland grades 2–4) from neurotmesis (Sunderland grade 5); therefore, imaging plays a key role in accurately grading the severity of nerve injury in these cases and ultimately dictating surgical management.

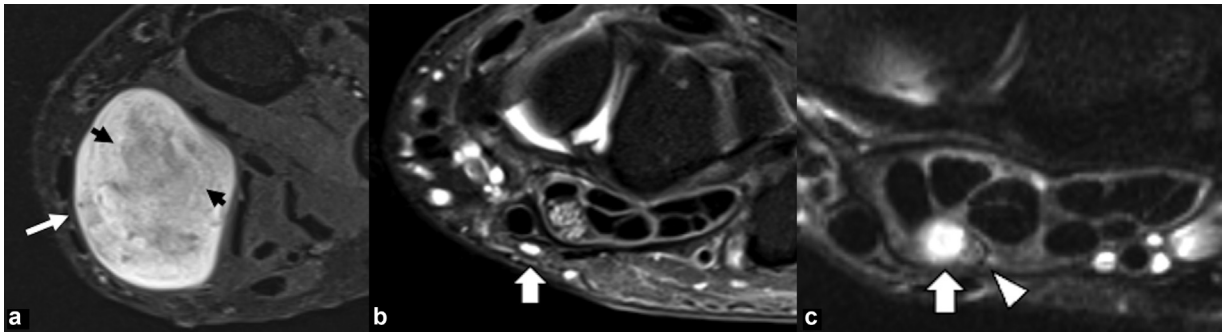

Fig. 12 Peripheral nerve sheath tumors. (**a**) Axial T2 fat-suppressed image in a 62-year-old woman with pain in the median neve distribution and palpable mass demonstrates a hyperintense mass in the expected location of the median nerve (white arrow). The mass contains areas of internal low to intermediate signal, likely representing fascicular bundles and referred to as the fascicular sign (black arrows). (**b**) Axial T2 fat-suppressed image in a 40-year-old woman with neurofibromatosis type 1 demonstrates focal hyperintense signal and enlargement of the palmar cutaneous branch of the median nerve consistent with a neurofibroma (white arrow). (**c**) Axial T2 fat-suppressed image in a 52-year-old woman with neurofibromatosis type 2 demonstrates a peripheral nerve sheath tumor involving selected fascicles of the median nerve (white arrow). Adjacent fascicles of the median nerve are normal (white arrowhead).

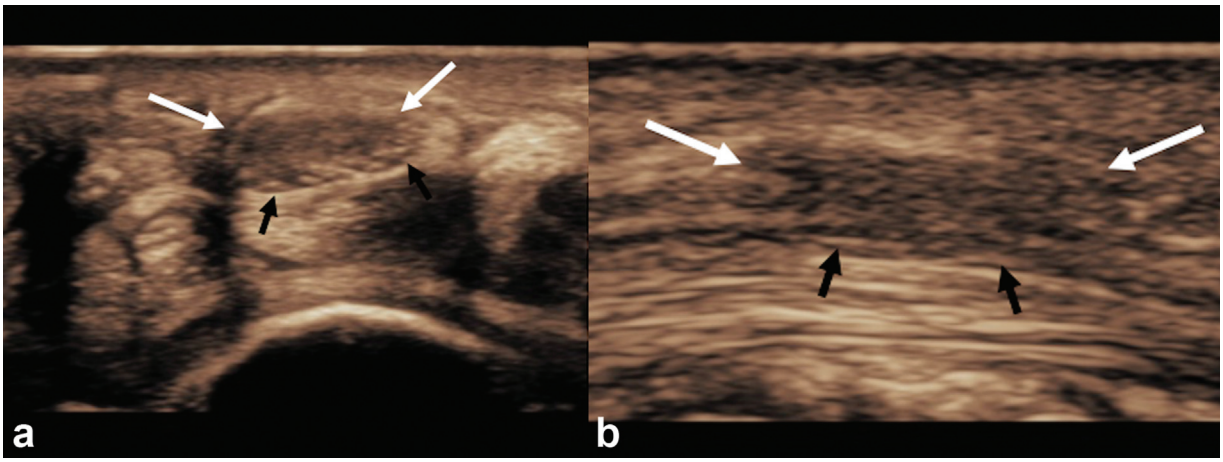

Fig. 13 A 43-year-old man with wrist laceration resulting in pain and numbness in the thumb. (**a**) Transverse ultrasonography (US) image of the median nerve demonstrates loss of the superficial fascicular architecture with focal nerve enlargement (white arrows). The deep nerve fascicles appear intact (black arrows). (**b**) Longitudinal US image similarly demonstrates focal enlargement of the hypoechoic superficial nerve consistent with a neuroma-in-continuity (white arrows). The deep fascicles are preserved (black arrows). Color Doppler image (not shown) showed no internal hypervascularity. The neuroma-in-continuity was treated with neuroma excision and allograft reconstruction.

The surgical treatment options for acute and subacute peripheral nerve injuries include direct end-to-end repair and nerve grafting (autografting or allografting) when bridging nerve defects. Artificial nerve conduits are an alternative to nerve grafting for the repair of short ($<$ 3 cm) sensory peripheral nerve defects. For complex and proximal peripheral nerve injuries, successful reinnervation via traditional nerve repair techniques remains challenging because of the long distance between the lesion and motor end plates. Axonal regeneration occurs at $\sim$ 1 mm/day, and motor end plates begin to undergo irreversible changes after 12 to 18 months of denervation. Even when treated promptly, these lesions incur a high risk of undergoing muscle atrophy before the regenerating axons can reach their target. Nerve transfers circumvent this issue by transferring a healthy expendable motor nerve in close proximity to the target muscle, to a more distal portion of the injured nerve, thus shortening the regeneration time.[75] Chronic peripheral motor nerve injuries not amenable to repair or nerve transfer are treated with tendon transfers.

Conclusion

Nerves of the wrist are involved in common causes of neuropathy, and imaging plays a key role in dictating patient management. Both US and MRI can be used to identify signs of compressive neuropathy, define masses along the course of nerves, and grade the severity of nerve injury in the setting of trauma. A thorough understanding of nerve anatomy and patterns of nerve injury is essential to identify nerve abnormalities in the wrist. This is especially important in cases where the clinical presentation makes it difficult to separate a distal nerve lesion from a proximal cause of neuropathic symptoms such as cervical radiculopathy or brachial plexopathy.

Conflict of Interest
None declared.

References

1 Doughty CT, Bowley MP. Entrapment neuropathies of the upper extremity. Med Clin North Am 2019;103(02):357–370
2 Saint-Lary O, Rébois A, Mediouni Z, Descatha A. Carpal tunnel syndrome: primary care and occupational factors. Front Med (Lausanne) 2015;2:28
3 Sneag DB, Arányi Z, Zusstone EM, et al. Fascicular constrictions above elbow typify anterior interosseous nerve syndrome. Muscle Nerve 2020;61(03):301–310
4 Stewart JD. Peripheral nerve fascicles: anatomy and clinical relevance. Muscle Nerve 2003;28(05):525–541
5 Sourkes M, Stewart JD. Common peroneal neuropathy: a study of selective motor and sensory involvement. Neurology 1991;41 (07):1029–1033
6 Haig AJ, Tzeng HM, LeBreck DB. The value of electrodiagnostic consultation for patients with upper extremity nerve complaints: a prospective comparison with the history and physical examination. Arch Phys Med Rehabil 1999;80(10):1273–1281
7 Brown JM, Yablon CM, Morag Y, Brandon CJ, Jacobson JA. US of the peripheral nerves of the upper extremity: a landmark approach. Radiographics 2016;36(02):452–463
8 Andreisek G, Crook DW, Burg D, Marincek B, Weishaupt D. Peripheral neuropathies of the median, radial, and ulnar nerves: MR imaging features. Radiographics 2006;26(05):1267–1287
9 Kästel T, Heiland S, Bäumer P, Bartsch AJ, Bendszus M, Pham M. Magic angle effect: a relevant artifact in MR neurography at 3T? AJNR Am J Neuroradiol 2011;32(05):821–827
10 Sanmugalingam N, Rault MEG, Toms AP. Normal variations in position and relations of the median nerve in the carpal tunnel: a cross-sectional observational study using clinical magnetic resonance imaging. Clin Anat 2020;33(04):598–604
11 Smith JL, Ebraheim NA. Anatomy of the palmar cutaneous branch of the median nerve: a review. J Orthop 2019;16(06):576–579
12 Lanz U. Anatomical variations of the median nerve in the carpal tunnel. J Hand Surg Am 1977;2(01):44–53
13 Petrover D, Bellity J, Vigan M, Nizard R, Hakime A. Ultrasound imaging of the thenar motor branch of the median nerve: a cadaveric study. Eur Radiol 2017;27(11):4883–4888

14 Bayrak IK, Bayrak AO, Kale M, Turker H, Diren B. Bifid median nerve in patients with carpal tunnel syndrome. J Ultrasound Med 2008;27(08):1129–1136
15 Shinagawa S, Tajika T, Oya N, et al. Prevalence of bifid median nerve and the cross-sectional area as assessed by ultrasonography in healthy Japanese subjects. J Hand Surg Global Online 2019; 1(02):74–78
16 Pierre-Jerome C, Smitson RD Jr, Shah RK, Moncayo V, Abdelnoor M, Terk MR. MRI of the median nerve and median artery in the carpal tunnel: prevalence of their anatomical variations and clinical significance. Surg Radiol Anat 2010;32(03):315–322
17 Gassner EM, Schocke M, Peer S, Schwabegger A, Jaschke W, Bodner G. Persistent median artery in the carpal tunnel: color Doppler ultrasonographic findings. J Ultrasound Med 2002;21 (04):455–461
18 Klauser AS, Halpern EJ, De Zordo T, et al. Carpal tunnel syndrome assessment with US: value of additional cross-sectional area measurements of the median nerve in patients versus healthy volunteers. Radiology 2009;250(01):171–177
19 Lee RKL, Griffith JF, Ng AWH, et al. Cross-sectional area of the median nerve at the wrist: comparison of sonographic, MRI, and cadaveric measurements. J Clin Ultrasound 2019;47(03): 122–127
20 Ng AWH, Griffith JF, Tong CSL, et al. MRI criteria for diagnosis and predicting severity of carpal tunnel syndrome. Skeletal Radiol 2020;49(03):397–405
21 Milone MT, Karim A, Klifto CS, Capo JT. Analysis of expected costs of carpal tunnel syndrome treatment strategies. Hand (N Y) 2019; 14(03):317–323
22 Ostergaard PJ, Meyer MA, Earp BE. Non-operative treatment of carpal tunnel syndrome. Curr Rev Musculoskelet Med 2020;13 (02):141–147
23 Patel K, Horak HA. Electrodiagnosis of common mononeuropathies: median, ulnar, and fibular (peroneal) neuropathies. Neurol Clin 2021;39(04):939–955
24 Witt JC, Hentz JG, Stevens JC. Carpal tunnel syndrome with normal nerve conduction studies. Muscle Nerve 2004;29(04): 515–522
25 Pan TJ, Byrne K, Fowler J. False positive rates of electrodiagnostic studies compared to ultrasound examination for carpal tunnel syndrome: level 4 evidence. J Hand Surg Am 2017;42(09):S9
26 Fowler JR, Munsch M, Tosti R, Hagberg WC, Imbriglia JE. Comparison of ultrasound and electrodiagnostic testing for diagnosis of carpal tunnel syndrome: study using a validated clinical tool as the reference standard. J Bone Joint Surg Am 2014;96(17):e148
27 Wong SM, Griffith JF, Hui ACF, Lo SK, Fu M, Wong KS. Carpal tunnel syndrome: diagnostic usefulness of sonography. Radiology 2004; 232(01):93–99
28 Ng AWH, Griffith JF, Lee RKL, Tse WL, Wong CWY, Ho PC. Ultrasound carpal tunnel syndrome: additional criteria for diagnosis. Clin Radiol 2018;73(02):214.e11–214.e18
29 Klauser AS, Abd Ellah MMH, Halpern EJ, et al. Sonographic cross-sectional area measurement in carpal tunnel syndrome patients: can delta and ratio calculations predict severity compared to nerve conduction studies? Eur Radiol 2015;25(08): 2419–2427
30 Klauser AS, Halpern EJ, Faschingbauer R, et al. Bifid median nerve in carpal tunnel syndrome: assessment with US cross-sectional area measurement. Radiology 2011;259(03):808–815
31 Gonzalez-Suarez CB, Fidel BC, Cabrera JTC, et al. Diagnostic accuracy of ultrasound parameters in carpal tunnel syndrome: additional criteria for diagnosis. J Ultrasound Med 2019;38(11): 3043–3052
32 Ooi CC, Wong SK, Tan ABH, et al. Diagnostic criteria of carpal tunnel syndrome using high-resolution ultrasonography: correlation with nerve conduction studies. Skeletal Radiol 2014;43 (10):1387–1394
33 Filler AG, Kliot M, Howe FA, et al. Application of magnetic resonance neurography in the evaluation of patients with peripheral nerve pathology. J Neurosurg 1996;85(02):299–309
34 Chen CH, Wu T, Sun JS, Lin WH, Chen CY. Unusual causes of carpal tunnel syndrome: space occupying lesions. J Hand Surg Eur Vol 2012;37(01):14–19
35 Pirola E, Hébert-Blouin MN, Amador N, Amrami KK, Spinner RJ. Palmaris profundus: one name, several subtypes, and a shared potential for nerve compression. Clin Anat 2009;22(06):643–648
36 Pfirrmann CWA, Zanetti M. Variants, pitfalls and asymptomatic findings in wrist and hand imaging. Eur J Radiol 2005;56(03): 286–295
37 Donnelly JP, Hanna M, Sperry BW, Seitz WH Jr. Carpal tunnel syndrome: a potential early, red-flag sign of amyloidosis. J Hand Surg Am 2019;44(10):868–876
38 Mosier BA, Hughes TB. Recurrent carpal tunnel syndrome. Hand Clin 2013;29(03):427–434
39 Ng AWH, Griffith JF, Tsoi C, et al. Ultrasonography findings of the carpal tunnel after endoscopic carpal tunnel release for carpal tunnel syndrome. Korean J Radiol 2021;22(07):1132–1141
40 Fadel ZT, Samargandi OA, Tang DT. Variations in the anatomical structures of the Guyon canal. Plast Surg (Oakv) 2017;25(02): 84–92
41 Blum AG, Zabel JP, Kohlmann R, et al. Pathologic conditions of the hypothenar eminence: evaluation with multidetector CT and MR imaging. Radiographics 2006;26(04):1021–1044
42 Reckelhoff KE, Li J, Kaeser MA, Haun DW, Kettner NW. Ultrasound evaluation of the normal ulnar nerve in Guyon's tunnel: cross-sectional area and anthropometric measurements. J Med Ultrasound 2015;23(04):171–176
43 Iyer VG. Ultrasonography in distal ulnar nerve neuropathy: findings in 33 patients. J Clin Neurophysiol 2021;38(02):156–159
44 Zeiss J, Jakab E, Khimji T, Imbriglia J. The ulnar tunnel at the wrist (Guyon's canal): normal MR anatomy and variants. AJR Am J Roentgenol 1992;158(05):1081–1085
45 Earp BE, Floyd WE, Louie D, Koris M, Protomastro P. Ulnar nerve entrapment at the wrist. J Am Acad Orthop Surg 2014;22(11): 699–706
46 Brubacher JW, Leversedge FJ. Ulnar neuropathy in cyclists. Hand Clin 2017;33(01):199–205
47 Gross MS, Gelberman RH. The anatomy of the distal ulnar tunnel. Clin Orthop Relat Res 1985;(196):238–247
48 Landau ME, Campbell WW. Clinical features and electrodiagnosis of ulnar neuropathies. Phys Med Rehabil Clin N Am 2013;24(01): 49–66
49 Campion D. Electrodiagnostic testing in hand surgery. J Hand Surg Am 1996;21(06):947–956
50 Kollmer J, Bäumer P, Milford D, et al. T2-signal of ulnar nerve branches at the wrist in Guyon's canal syndrome. PLoS One 2012; 7(10):e47295
51 Ruocco MJ, Walsh JJ, Jackson JP. MR imaging of ulnar nerve entrapment secondary to an anomalous wrist muscle. Skeletal Radiol 1998;27(04):218–221
52 Claassen H, Schmitt O, Schulze M, Wree A. Variation in the hypothenar muscles and its impact on ulnar tunnel syndrome. Surg Radiol Anat 2013;35(10):893–899
53 Harvie P, Patel N, Ostlere SJ. Prevalence and epidemiological variation of anomalous muscles at Guyon's canal. J Hand Surg [Br] 2004;29(01):26–29
54 Waugh RP, Pellegrini VD Jr. Ulnar tunnel syndrome. Hand Clin 2007;23(03):301–310, v
55 Murata K, Shih JT, Tsai TM. Causes of ulnar tunnel syndrome: a retrospective study of 31 subjects. J Hand Surg Am 2003;28(04): 647–651
56 Feldman MD, Rotman MB, Manske PR. Compression of the deep motor branch of the ulnar nerve by a midpalmar ganglion. Orthopedics 1995;18(01):65–67

57 Duggal A, Anastakis DJ, Salonen D, Becker E. Compression of the deep palmar branch of the ulnar nerve by a ganglion : a case report. Hand (N Y) 2006;1(02):98–101
58 Marx SC, Dhalapathy S, Marx CA, Babu MS, Pulakunta T, Vasanthakumar S. Ultrasonographical and histological cross-sectional study of the human superficial branch of the radial nerve. Rom J Morphol Embryol 2011;52(3, Suppl):1081–1090
59 Kim KH, Byun EJ, Oh EH. Ultrasonographic findings of superficial radial nerve and cephalic vein. Ann Rehabil Med 2014;38(01): 52–56
60 Zwart K, Roeling TAP, van Leeuwen WF, Schuurman AH. An anatomical study to the branching pattern of the posterior interosseous nerve on the dorsal side of the hand. Clin Anat 2020;33(05):678–682
61 Rizzo M, Berger RA, Steinmann SP, Bishop AT. Arthroscopic resection in the management of dorsal wrist ganglions: results with a minimum 2-year follow-up period. J Hand Surg Am 2004; 29(01):59–62
62 Lanzetta M, Foucher G. Entrapment of the superficial branch of the radial nerve (Wartenberg's syndrome). A report of 52 cases. Int Orthop 1993;17(06):342–345
63 Dang AC, Rodner CM. Unusual compression neuropathies of the forearm, part I: radial nerve. J Hand Surg Am 2009;34(10): 1906–1914
64 Grant AC, Cook AA. A prospective study of handcuff neuropathies. Muscle Nerve 2000;23(06):933–938
65 De Maeseneer M, Marcelis S, Jager T, Girard C, Gest T, Jamadar D. Spectrum of normal and pathologic findings in the region of the first extensor compartment of the wrist: sonographic findings and correlations with dissections. J Ultrasound Med 2009;28 (06):779–786
66 Silverman TA, Enzinger FM. Fibrolipomatous hamartoma of nerve. A clinicopathologic analysis of 26 cases. Am J Surg Pathol 1985;9(01): 7–14
67 Toms AP, Anastakis D, Bleakney RR, Marshall TJ. Lipofibromatous hamartoma of the upper extremity: a review of the radiologic findings for 15 patients. AJR Am J Roentgenol 2006;186(03): 805–811
68 Marom EM, Helms CA. Fibrolipomatous hamartoma: pathognomonic on MR imaging. Skeletal Radiol 1999;28(05):260–264
69 Reynolds DL Jr, Jacobson JA, Inampudi P, Jamadar DA, Ebrahim FS, Hayes CW. Sonographic characteristics of peripheral nerve sheath tumors. AJR Am J Roentgenol 2004;182(03):741–744
70 Kakkar C, Shetty CM, Koteshwara P, Bajpai S. Telltale signs of peripheral neurogenic tumors on magnetic resonance imaging. Indian J Radiol Imaging 2015;25(04):453–458
71 Noble J, Munro CA, Prasad VS, Midha R. Analysis of upper and lower extremity peripheral nerve injuries in a population of patients with multiple injuries. J Trauma 1998;45(01):116–122
72 Sunderland S. A classification of peripheral nerve injuries producing loss of function. Brain 1951;74(04):491–516
73 Grinsell D, Keating CP, Keating CP. Peripheral nerve reconstruction after injury: a review of clinical and experimental therapies. BioMed Res Int 2014;2014:698256
74 Campbell WW. Evaluation and management of peripheral nerve injury. Clin Neurophysiol 2008;119(09):1951–1965
75 Dvali L, Mackinnon S. Nerve repair, grafting, and nerve transfers. Clin Plast Surg 2003;30(02):203–221